

# PHYSICAL REVIEW LETTERS

VOLUME 36

3 MAY 1976

NUMBER 18

## Diffusive Phenomena in the Charge and Angular Distributions for the Reaction



L. G. Moretto,\* B. Cauvin,‡ P. Glässel, R. Jared, P. Russo, J. Sventek, and G. Wozniak  
*Lawrence Berkeley Laboratory and Department of Chemistry, University of California,*

*Berkeley, California 94720*

(Received 2 February 1976)

The cross sections and the kinetic energy distributions of fragments with individually resolved atomic numbers have been measured as a function of angle. The variations in the  $Z$  distribution widths with angle and the change of the angular distributions from side peaked for  $Z$ 's close to 36 to forward peaked for  $Z$ 's far removed from 36 dramatically demonstrates the presence of diffusion of nucleons between the target and projectile.

Recently both the  $Z$  and angular distributions have been measured for the deep-inelastic component associated with the N-, Ne-, and Ar-induced reactions.<sup>1-4</sup> While in these experiments the  $Z$  distributions are only indicative of incomplete equilibration of the mass- and charge-asymmetry degree of freedom, the angular distributions as a function of  $Z$  clearly indicate a progressive delay for the emission of the particles farther removed in  $Z$  from the projectile. This was inferred from the forward peaking of the angular distributions (in excess of  $1/\sin\theta$ ) which progressively disappears for fragments farther removed in  $Z$  from the projectile. On the basis of this evidence,<sup>1-5</sup> Moretto and Sventek<sup>6</sup> proposed a diffusion model which quantitatively accounts for the observed features.

In apparent contrast with the above experiments, the reaction products from Kr on heavy targets show a marked side peaking in the gross angular distribution (all products taken simultaneously) of the quasi-fission peak.<sup>7,8</sup> Furthermore, coarse mass distributions (measured at a few angles) appear to be narrowly peaked around the projectile.<sup>7,8</sup>

In order to ascertain whether the differences observed in these two groups of reactions are

due to different mechanisms, or alternatively, represent different aspects of the same process, a detailed study of the reaction Au + Kr at 620-MeV bombarding energy was undertaken. As an improvement on previous experiments, a gas  $\Delta E$ , solid-state  $E$  telescope, developed by our group,<sup>9</sup> was used which resolved individual atomic numbers up to  $\sim Z = 50$ . A self-supporting Au foil (0.80 mg/cm<sup>2</sup>) was bombarded with a 620-MeV Kr beam from the Berkeley SuperHILAC which delivered beam intensities ranging from 10 to 100 nA (charge) on target. The two independent arms in the scattering chamber each supported two  $\Delta E$ - $E$  telescopes, separated by 15° or 20°.

The data were analyzed off-line on a PDP-9 computer. The data were transformed to the center-of-mass system by assuming for each  $Z$  a mass ratio such that the liquid-drop energy of the two touching spheres is minimized with respect to the charge ratio.

The center-of-mass kinetic energy distributions were inspected for the presence of an identifiable quasi-elastic component, which would then be subtracted, when possible, from the total spectrum. Close to the grazing angle and for  $Z$ 's close to the projectile, these two components could not be decomposed and the integration of the relaxed

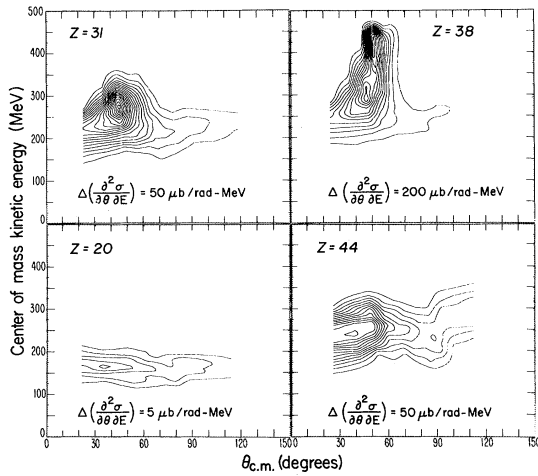


FIG. 1. Contour plots of  $\partial^2\sigma/\partial E \partial\theta$  in the  $E_{c.m.}, \theta_{c.m.}$  plane for various atomic numbers.

component was omitted.

The data are displayed in three forms: (i) For each  $Z$  a contour map of  $\partial^2\sigma/\partial E \partial\theta$  is generated in the  $E_T, \theta_{c.m.}$  plane,  $E_T$  being the total kinetic energy associated with the exit channel. Examples of these contour plots are given in Fig. 1. (ii) The laboratory cross sections  $d\sigma/d\Omega$  versus  $Z$  at various laboratory angles are displayed in Fig. 2. (iii) The center-of-mass cross sections  $d\sigma/d\Omega$  for each  $Z$  are plotted versus center-of-mass angle in Fig. 3.

In Fig. 1 the quasi-elastic and the relaxed peaks are seen for  $Z$ 's close to 36. For fragments farther removed in  $Z$  from 36, the quasi-elastic peak degenerates into a high-energy tail which eventually disappears. At all angles the relaxed peak has an energy fairly close to the calculated Coulomb energies of two spheres. The widths of the kinetic energy distributions are essentially constant both with  $Z$  and with angle ( $\sim 50$  MeV full width at half-maximum). For angles close to the grazing angle and for  $Z$ 's close to 36, one cannot verify the above statements because of the presence of large quasi-elastic peaks.

In Fig. 2 the  $Z$  distributions are presented for various laboratory angles. At intermediate angles ( $\theta_L \approx 40^\circ$ ) the distributions are narrow and sharply peaked about  $Z=36$ . The cross section falls off more rapidly in the low- $Z$  than in the high- $Z$  region. At more backward angles the distributions are substantially broader, and the cross sections remain constant over a fairly large number of  $Z$ 's near the peak of the distribution. The centroid appears to be shifted to-

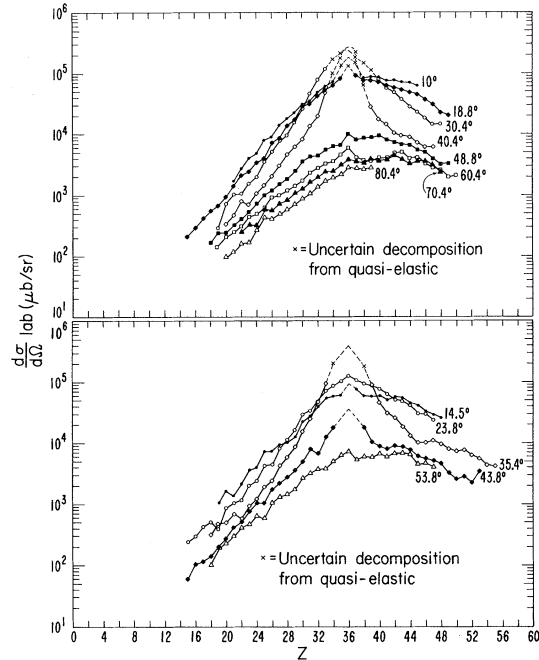


FIG. 2. Laboratory  $Z$  distributions ( $d\sigma/d\Omega$ ) for various laboratory angles.

wards higher  $Z$ 's and the falling off in the high- $Z$  region is not very marked. At the most forward angles the distributions are also broader than those observed at intermediate angles, but less broad than those observed at the more backward angles.

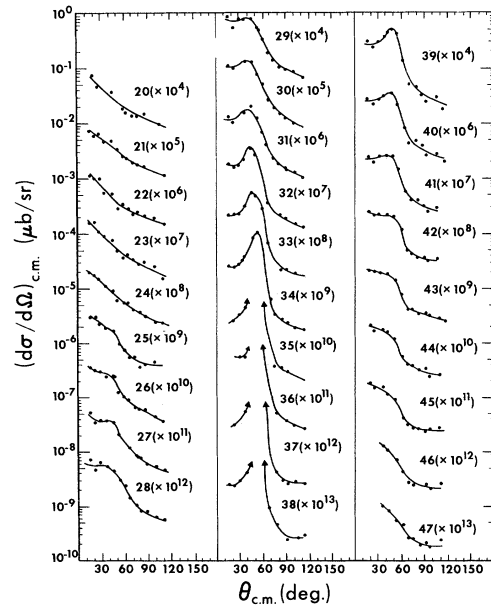


FIG. 3. Center-of-mass angular distributions for various atomic numbers.

The change in the distributions from narrow to broad can be interpreted as due to the diffusion along the mass-asymmetry coordinate of the "intermediate complex."<sup>5,6</sup> It appears that the narrow distributions are relatively "young" and should be associated with short interaction times, because diffusion has not had time to randomly exchange many particles. On the same basis, broader distributions can be considered older and associated with longer interaction times. Similarly the shift or drift of the centroid toward higher  $Z$ 's is the result of a diffusion process governed by the potential energy of the intermediate complex which favors the exchange of particles in the direction of symmetry. Again the drift is more visible in the broader or older distributions.

A somewhat puzzling feature is observed in the relationship between the "age" of a distribution in  $Z$  and the angular range at which it is observed. In fact, one notices a peculiar inversion: Old distributions are observed at the broader angles, young distributions at intermediate angles, and middle-aged distributions at forward angles.

If one assumes that the lifetime of the intermediate complex decreases rapidly with increasing impact parameter, the above feature can be qualitatively understood as an impact-parameter effect. The distributions observed at the larger angles appear to be associated with small impact parameters or near head-on collisions. Although the intermediate complex lives the longest, the angular velocity is so small that the decay products do not reach too far forward. For the intermediate impact parameters the collision angle is larger, the intermediate complex rotates faster, and the lifetimes are not too short, so that the products reach very forward angles. Finally, at the largest impact parameters, although the collision occurs quite peripherally, thus forming rapidly rotating complexes, the decay occurs so quickly that the fragments actually are emitted at angles not quite as forward as are those associated with intermediate impact parameters.

Figure 3 shows the center-of-mass angular distributions for the various  $Z$ 's. These angular distributions are side peaked ( $\sim 40^\circ$ ) for  $Z$ 's close to the projectile. As one moves away from  $Z=36$ , towards both lower and higher  $Z$ 's, the small-angle cross section increases with respect to the peak of the angular distribution. Therefore the side peaking evolves first into a shoulder and then disappears entirely, leaving angular distributions which are generally forward peaked and

similar to those observed in Ne- and Ar-induced reactions (see also Fig. 1).

Also these features can be qualitatively explained in terms of a diffusion model. For  $Z \approx 36$  the decay time is so short that no fragment reaches  $0^\circ$ , thus resulting in a side peaking. Fragments with  $Z$  progressively larger or smaller than 36 are populated by diffusion on a progressively longer time scale. This results in a selection of progressively larger lifetimes. The complex can then rotate more forward and actually some fragments begin being emitted close or even beyond  $0^\circ$ , giving rise to the transformation of the side peak into a shoulder. At very large distances in  $Z$  from the projectile, the lifetimes become so long that the complex succeeds in rotating past  $0^\circ$ . This partial orbiting is sufficient to generate a sharply forward-peaked angular distribution.

In conclusion, it appears that in the same experiment a natural and continuous connection is seen between the side-peaked angular distributions and the forward-peaked angular distributions, typical of the reactions with lighter ions.

This evidence, on one hand, supports the general predictions of the diffusion model, and on the other, it offers the possibility of studying diffusion times and decay times as a function of the impact parameter.

---

†This work done under the auspices of the U. S. Energy Research and Development Administration.

\*Alfred P. Sloan Foundation Fellow 1974-1976.

‡On leave from Département de Physique Nucléaire à Moyennes Energies, Centre d'Etudes Nucléaires, Saclay, France.

<sup>1</sup>L. G. Moretto, S. K. Kataria, R. C. Jared, R. Schmitt, and S. G. Thompson, Nucl. Phys. **A255**, 491 (1975).

<sup>2</sup>J. Galin, L. G. Moretto, R. Babinet, R. Schmitt, R. Jared, and S. G. Thompson, Nucl. Phys. **A255**, 472 (1975).

<sup>3</sup>R. Babinet, L. G. Moretto, J. Galin, R. Jared, J. Moulton, and S. G. Thompson, Nucl. Phys. **A258**, 172 (1976).

<sup>4</sup>L. G. Moretto, J. Galin, R. Babinet, Z. Fraenkel, R. Schmitt, R. Jared, and S. G. Thompson, Lawrence Berkeley Laboratory Report No. LBL-4084 (to be published).

<sup>5</sup>L. G. Moretto, R. P. Babinet, J. Galin, and S. G. Thompson, Phys. Lett. **58B**, 31 (1975).

<sup>6</sup>L. G. Moretto and J. S. Sventek, Phys. Lett. **58B**, 26 (1975).

<sup>7</sup>F. Hanappe, M. Lefort, C. Ngô, J. Péter, and

B. Tamain, Phys. Rev. Lett. **32**, 738 (1974).

<sup>8</sup>K. L. Wolf, J. P. Unik, J. R. Huizenga, J. R. Birkenlund, H. Freiesleben, and V. E. Viola, Phys. Rev. Lett.

**33**, 1105 (1974).

<sup>9</sup>M. M. Fowler and R. C. Jared, Nucl. Instrum. Methods **124**, 341 (1975).

## Magnetic Moment of the $6^+$ Isomeric State of $^{134}\text{Te}^\dagger$

A. Wolf\* and E. Cheifetz

*Department of Nuclear Physics, Weizmann Institute of Science, Rehovot, Israel*

(Received 4 March 1976)

The inherent alignment of the prompt fission fragments was used to measure the  $g$  factor of the  $6^+$  isomeric state of  $^{134}\text{Te}$  by the time-differential perturbed angular-correlation method. The experimental result  $g_{\text{exp}} = 0.846 \pm 0.025$  is close to effective  $g$  factors of  $g_{7/2}$  protons in nuclei with 82 neutrons. The deviation from the Schmidt value is discussed in terms of the polarization of the  $^{182}_{50}\text{Sn}_{82}$  core by the  $g_{7/2}$  protons.

Angular distributions of specific  $\gamma$  rays emitted in the ground-state bands of even-even fragments from spontaneous fission of  $^{252}\text{Cf}$  were found<sup>1,2</sup> to be peaked in the direction of the fission fragments with an average anisotropy of  $N(0^\circ)/N(90^\circ) = 1.50$ ,<sup>2</sup> thus showing alignment of the angular momentum of the fragments in a plane normal to the fission direction. In this work, we show that the inherent alignment of the fission fragments can be used for  $g$ -factor measurements. Specifically, the magnetic moment of the  $6^+$  isomeric state in  $^{134}\text{Te}$  has been determined by a time-differential perturbed-angular-correlation measurement.

The isotope  $^{134}\text{Te}$  has two protons outside the  $^{132}_{50}\text{Sn}_{82}$  core which is the only accessible double magic nucleus between  $^{56}\text{Ni}$  and  $^{208}\text{Pb}$ . This isotope lies far from the  $\beta$ -stability line on the neutron-rich side in a region of nuclei that have been reached solely through fission of actinides.  $^{134}\text{Te}$  has a  $6^+$  isomeric state ( $T_{1/2} = 163$  nsec) at 1691 keV, decaying by an  $E2$ , 115.3-keV transition to a  $4^+$  state and subsequently by a  $4^+ \rightarrow 2^+ \rightarrow 0^+$  cascade to the ground state. It was identified both in experiments involving isomeric decay of prompt fission products,<sup>3,4</sup> and in  $\beta$  decay of the mass separated  $A = 134$  chain.<sup>5</sup> This state is believed<sup>6,7</sup> to be composed predominantly of the  $\pi(g_{7/2})^2$  configuration, with the two protons coupled to maximum angular momentum.

We have measured, in an experiment described elsewhere,<sup>2</sup> the angular distribution of the 115.3-keV,  $6^+ \rightarrow 4^+$  transition in  $^{134}\text{Te}$  with respect to the fission direction and found it to be

$$W(\theta) = 1 + (0.25 \pm 0.09)P_2(\cos\theta) - (0.17 \pm 0.11)P_4(\cos\theta).$$

The yield of this transition,  $(60 \pm 4) \times 10^{-4}$  photons per fission,<sup>3,4</sup> is large enough to permit a time-differential measurement.

The experimental setup is shown schematically in Fig. 1. A thin,  $10^7$  fissions/min,  $^{252}\text{Cf}$  source having an active area of  $3 \text{ mm}^2$ , and plated on a copper foil of  $25 \text{ mg/cm}^2$  thickness was placed in a magnetic field of  $7.57 \pm 0.15 \text{ kG}$  normal to the plane of Fig. 1.  $\gamma$  rays emitted by fragments stopped in the copper backing at three angles ( $45^\circ$ ,  $0^\circ$ ,  $-45^\circ$ ) with respect to the fission axis were detected in a planar 2-cm<sup>3</sup> Ge(Li) detector. The fission direction was determined by the complementary fragments which were detected in any one of three surface-barrier detectors. A multi-parameter experiment was performed in which the kinetic energy of the fission fragments, the  $\gamma$ -ray energy, and the time difference between detection of a fission fragment and a  $\gamma$  ray were simultaneously recorded on magnetic tape. The time resolution, after correction for walk, was 10 nsec full width at half-maximum (FWHM) at

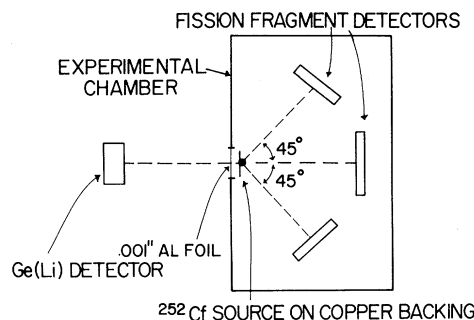


FIG. 1. Schematic description of the experimental system.